

Z-Spec: a broadband, direct-detection, millimeter-wave spectrometer

Bret J. Naylor^{1§}, Peter A. R. Ade², James J. Bock^{1,3}, C. Matt Bradford¹, Mark Dragovan³,
Lionel Duband⁴, Lieko Earle⁵, Jason Glenn⁵, Hideo Matsuhara⁶, Hien Nguyen³, Minhee Yun³,
Jonas Zmuidzinas¹

¹California Institute of Technology, Pasadena, CA

²Department of Physics and Astronomy, University of Wales, Cardiff, UK

³Jet Propulsion Laboratory, Pasadena, CA

⁴SBT, Commissariat à l'Énergie Atomique, Grenoble, France

⁵CASA, University of Colorado, Boulder, CO

⁶Institute of Space and Astronautical Science, Sagami, Japan

ABSTRACT

Z-Spec is a broadband (195 - 310 GHz), direct-detection, millimeter-wave spectrometer with moderate resolution ($R \sim 350$) that we are building to observe CO rotational lines and atomic fine-structure lines in the recently discovered population of submillimeter galaxies. A large fraction of these sources cannot be identified optically and thus redshift determination is extremely difficult. The large instantaneous bandwidth of Z-Spec will allow measurement of redshifts up to $z \sim 4$ via detection of two or more CO lines in a single spectrum. The spectrometer is based on a parallel-plate waveguide grating architecture that is substantially more compact than a conventional free-space grating system. The spectrometer and an array of 160 silicon nitride micromesh bolometers will be cooled to 100 mK to provide background-limited sensitivity. In addition to measuring the redshifts of sources discovered in submillimeter continuum surveys, Z-Spec will demonstrate a novel spectrometer concept well-suited for future far-infrared space missions.

Keywords: millimeter-wave, spectroscopy, bolometers, cryogenic, waveguide, diffraction grating

1. INTRODUCTION

Decoding far-infrared emission is crucial to understanding the processes of galaxy formation and active galactic nuclei. The COBE satellite discovered an extra-galactic far-infrared background^{1,2,3}, which has been partially resolved by large format submillimeter cameras, such as SCUBA⁴. These instruments have detected a couple hundred galaxies and many more will be detected when the next generation of far-infrared and millimeter-wave imagers become available (e.g. SIRTf, Bolocam, SHARC II, ASTRO-F, HAWC, SCUBA-2, Herschel). Follow-up observation of this new population of submillimeter galaxies has been difficult because of the challenges in finding radio or optical counterparts to the submillimeter sources. Due to the strong negative-K correction in the submillimeter band, many of these objects could have high redshifts ($z > 1$). A broadband, millimeter or submillimeter, moderate-resolution spectrometer is needed to measure the redshifts of these galaxies.

A properly designed direct-detection system is potentially more sensitive at these wavelengths than a heterodyne system because of the additional quantum noise in the mixer. The advantage of direct detectors increases when the backgrounds are small, for example in the case of a cooled space-borne telescope. Furthermore, assuming equivalent optical efficiencies, a diffraction grating is better for line surveys over a large spectral band than a Fourier Transform Spectrometer (FTS) or a Fabry-Perot system because of the increased photon background noise on the detector(s) in an FTS and the scanning penalty of a Fabry-Perot. If the path-folding advantages of an FTS or Fabry-Perot are eliminated in favor of sensitivity and instantaneous bandwidth afforded by a diffraction grating, the grating

[§] For further information contact Bret Naylor, e-mail: naylor@submm.caltech.edu, phone: 1 (626) 395-2601.

system can get prohibitively large for even moderate spectral resolution. However, using a grating in parallel-plate waveguide can significantly reduce the required volume.

We are building Z-Spec, a broadband, direct-detection spectrometer that will measure redshifts of submillimeter galaxies from the Caltech Submillimeter Observatory (CSO). It is based on the Waveguide Far-Infrared Spectrometer (WaFIRS) diffraction grating design⁵, which uses the Rowland grating geometry in a parallel-plate waveguide. Z-Spec is designed to measure redshifts by using the ladder of CO rotational transitions. Z-Spec will instantaneously cover all of the 1 mm atmospheric window and will be capable of measuring two or more CO lines simultaneously, which are spaced by $115/(1+z)$ GHz in the observed frame, for all $z > 0.9$. For redshifts below that, one or two candidate redshifts can be obtained from a single line. Z-Spec is also capable of performing millimeter-wave line surveys of nearby galaxies. Its large bandwidth and high sensitivity will enable rapid measurement of redshifts and line luminosities, providing the basis for detailed follow-up observations with higher spatial and spectral resolution instruments.

Additionally, Z-Spec will demonstrate a new spectrometer architecture which is useful for future space-borne telescopes. The upcoming SIRTf, ASTRO-F and HSO missions will map the far-infrared sky and measure continuum source counts to their confusion limits, revealing many thousands of galaxies. Most of the discovered sources, however, will be below the sensitivity limits of the spectrometers onboard these telescopes. Future space missions will be needed to follow-up the imaging surveys with sensitive broad-band spectroscopy in order to measure redshifts and interstellar medium conditions. A key problem is that current spectrometer designs are either too complicated or too large when scaled into the far-infrared or submillimeter. Because it is much more compact than conventional systems, Z-Spec is the first implementation of a new technology which could be well-suited to far-infrared spectroscopy from space.

2. DESIGN OVERVIEW

Z-Spec will initially be used on the 10.4 m CSO telescope in a single-beam, single-polarization configuration. It makes full use of the 1 mm atmospheric window. The designed resolving power varies from 400 at 1.54 mm to 250 at 0.97 mm for a grating with 480 facets. To achieve high sensitivity, 160 Si_3N_4 micromesh bolometers will be waveguide-coupled to the WaFIRS grating in Z-Spec. The grating and detectors will be cooled to 100 mK to enable background-limited performance at the CSO. The cooling is provided by an adiabatic demagnetization refrigerator (ADR) in a standard liquid nitrogen and liquid helium dewar. The ADR is backed by a two-stage helium sorption refrigerator. We will use the mature readout electronics design from Bolocam⁶. Initially, the instrument will chop on the sky, though eventually a second WaFIRS module could be added to double the on-source duty cycle or to observe both polarizations.

Z-Spec will receive light from the telescope with a corrugated feed horn, which tapers down to single-mode rectangular waveguide. The light is filtered with a series of metal-mesh filters to reject out-of-band radiation. The single-mode waveguide connects to the spectrometer input horn which gently tapers in both height and width. Light enters the parallel-plate waveguide via the input and reflects off the diffraction grating. Different frequencies focus to different points along a circular arc where rectangular waveguides receive the radiation and couple it to individually mounted bolometers (see Figure 1). The bolometer signals are amplified by matched pairs of J-FETs inside the dewar and then brought out to the warm electronics.

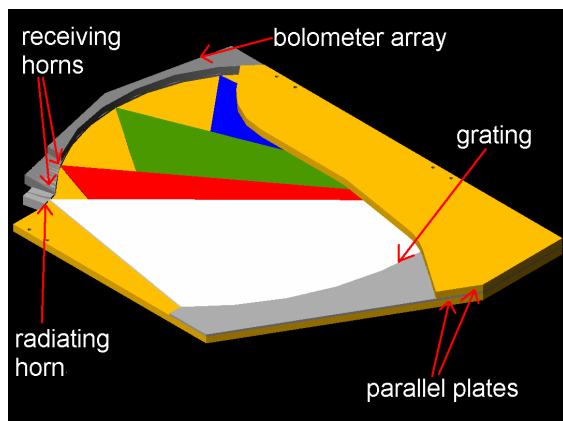


Figure 1: A schematic of the WaFIRS spectrometer concept shown with the top plate partially cut away. A back-to-back feedhorn receives radiation from the telescope (left) and transmits it onto the faceted grating surface (bottom). The curved grating focuses the spectrally-dispersed light onto the array of receiving feed horns and bolometers (upper left). Three beams of dispersed “colors” from the incoming “white” light are shown.

3. WAVEGUIDE DIFFRACTION GRATING

The inherent sensitivity advantages of diffraction grating spectroscopy led us to explore the possibility of building a three-dimensional grating system, but it required a $90\text{ cm} \times 75\text{ cm} \times 75\text{ cm}$ cryogenic volume for the optics alone to achieve a resolving power of 300. A significant savings in volume can be achieved by placing the grating in a parallel-plate waveguide. Furthermore, the use of a curved grating allows a single powered surface to simultaneously disperse and focus the radiation, eliminating the need for other optical elements. This allows the size of the grating to drive the size of the instrument, resulting in a very space efficient design. The WaFIRS module in Z-Spec will be $62\text{ cm} \times 48\text{ cm} \times 3.3\text{ cm}$.

The parallel-plate waveguide propagates a single electromagnetic mode (TE_1) polarized parallel to the plates. It has a half-wave vertical electric field intensity profile that vanishes at the top and bottom plates. Radiation is injected into the parallel plate medium with a feedhorn that provides a suitable illumination pattern on the grating. The illumination of the grating affects the spectral resolution and the optical efficiency. A larger beam from a smaller input horn produces higher spectral resolution, but lower efficiency because power is lost beyond the edges of the grating as spillover. The Z-Spec grating works in first order and disperses the radiation onto a circular focal curve, which extends over nearly 90° of arc. Waveguide bend blocks at this focal surface transmit the dispersed radiation of adjacent channels either up or down to waveguide-coupled bolometers (see Figure 2).

The grating facets are positioned such that two frequencies on opposite ends of the band have changes in the input-to-output propagation phase of 2π from one facet to the next. This provides perfect (stigmatic) performance at these two frequencies. If the two stigmatic frequencies are properly chosen, the aberrations for other frequencies remain smaller than the diffraction limit. Hence, the grating is diffraction limited over its full band. The blaze efficiency is $> 90\%$ across the band, based on a calculation for plane gratings using PCGrate, a commercially available simulation package.

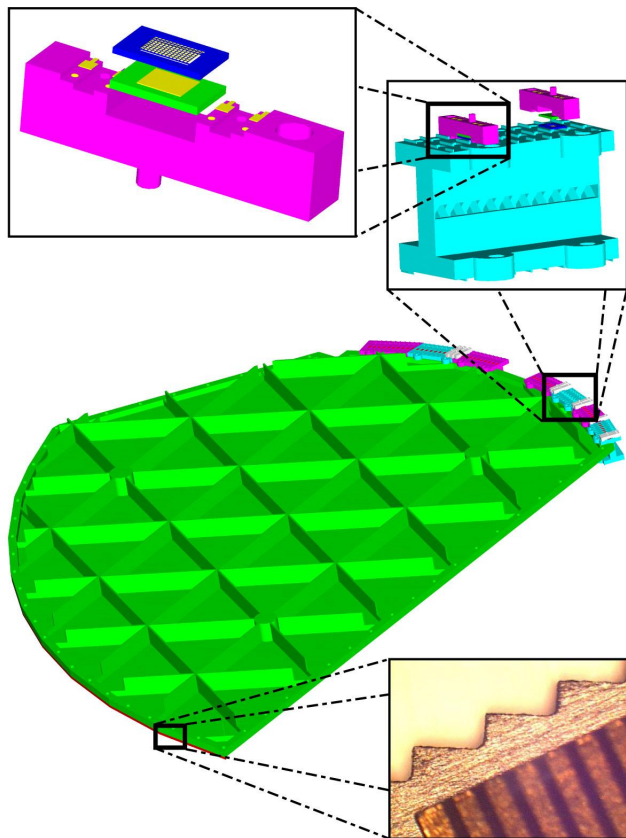


Figure 2: The grating is shown in the center with light-weighting on the exterior visible. The lower right panel is a photograph of the prototype blazed surface. Each facet (cut by wire EDM) is approximately 1 mm wide. Above and to the right is a schematic drawing of a mitred waveguide bend block. Radiation enters along the middle and is reflected up and down alternately in adjacent channels. The upper-left drawing is a single bolometer module with a backshort and bolometer shown.

To evaluate and optimize the Z-Spec grating design, we performed diffraction calculations that included the amplitude and phase produced by the radiating horn at each facet. Reflected contributions from each facet were summed for each output location along the focal arc, accounting for phase and amplitude changes due to propagation through the waveguide. The resulting line profiles were calculated for each frequency along the focal curve. We used these simulations to select optimal stigmatic points, optimize the aperture and orientation of the spectrometer input horn, and calculate the size and orientation of the waveguide output feeds.

The parallel plate separation was chosen to minimize the waveguide loss ($\text{loss} \propto (\Delta y)^{-3}$ for a separation of Δy) and to maximize coupling of the radiation to the waveguide output feeds, which favors a small Δy . Large separations can excite higher-order modes that do not couple as efficiently to the waveguide feeds as the fundamental mode. The horizontal spot sizes produced by the grating are $(1-2)\lambda$ in size. Taken together, these considerations dictated a 2.5 mm spacing for our millimeter-wave system with an expected parallel plate waveguide loss of $<3\%$ at 100 mK for polished, gold-plated aluminum plates.

We built and tested a warm prototype grating that was slightly smaller than the Z-Spec instrument. Its grating has 400 facets with a 29° blaze angle and an expected resolving power varying from 250 at 1.54 mm to 180 at 0.98 mm (Figure 3). We tested it using a backwards-wave oscillator which provided a sweepable source in waveguide. This signal was fed into the spectrometer with an input horn which tapered up from single mode waveguide and radiated into the parallel plate region. Power was gathered on the focal arc with a feed horn that could be mounted at any location. This receiving horn tapered down to a single-mode waveguide and coupled to a Shottky diode detector for power measurement.

For the measurements plotted in Figure 4, two output horns were used. Both had sizes comparable to the diffraction spot, but they were oriented at different angles with respect to the focal arc. For most frequencies, neither of these two horns was well-matched to the beams, and the coupling was less than would be achieved with horns designed for each frequency. Since the diode detector only coupled a single mode, it did not measure all of the power that arrived in the diffraction spots. The optimized system will use multi-mode feeds, each tuned for its frequency and position on the focal curve, and multi-mode detectors, eliminating these two sources of loss which were present in our test setup.

To correct for the inefficiencies from the non-optimum horns, we measured the shapes of the profiles at a few frequencies with a very small feed horn. The spectral resolution results are quite close to our predictions over much of the band. With the profile known, the fractional response of the larger output due to the imperfectly matched horn was calculated, and the measurements corrected. These are the lighter, upper curves for each line in Figure 4. Accounting for this coupling inefficiency produced the corrected curves which are close to the predicted performance. It was limited by waveguide propagation loss, spillover loss, and grating efficiency indicated by the modeled performance envelope. The high-frequency degradation is due to a blaze inefficiency, which will be corrected for in Z-Spec. The ideal cryogenic system accounts for the reduction in waveguide loss when the system is cooled from room temperature to 100 mK.

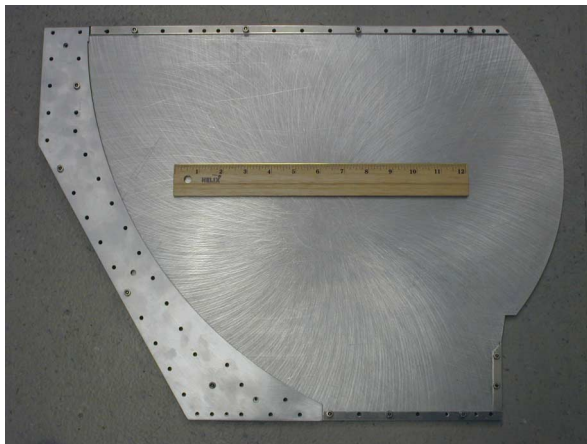


Figure 3: Z-Spec prototype grating with one plate removed. The blazed surface is on the left. Assembled, the grating is 56 cm \times 42 cm \times 2.25 cm. A 12-inch ruler is shown for scale. The input horn is attached on the lower right, just below the curved focal arc. The output feed can be attached anywhere along the arc on the right side of the plate. Lower frequencies are focused close to the input horn, with higher frequencies arriving higher along the curve.

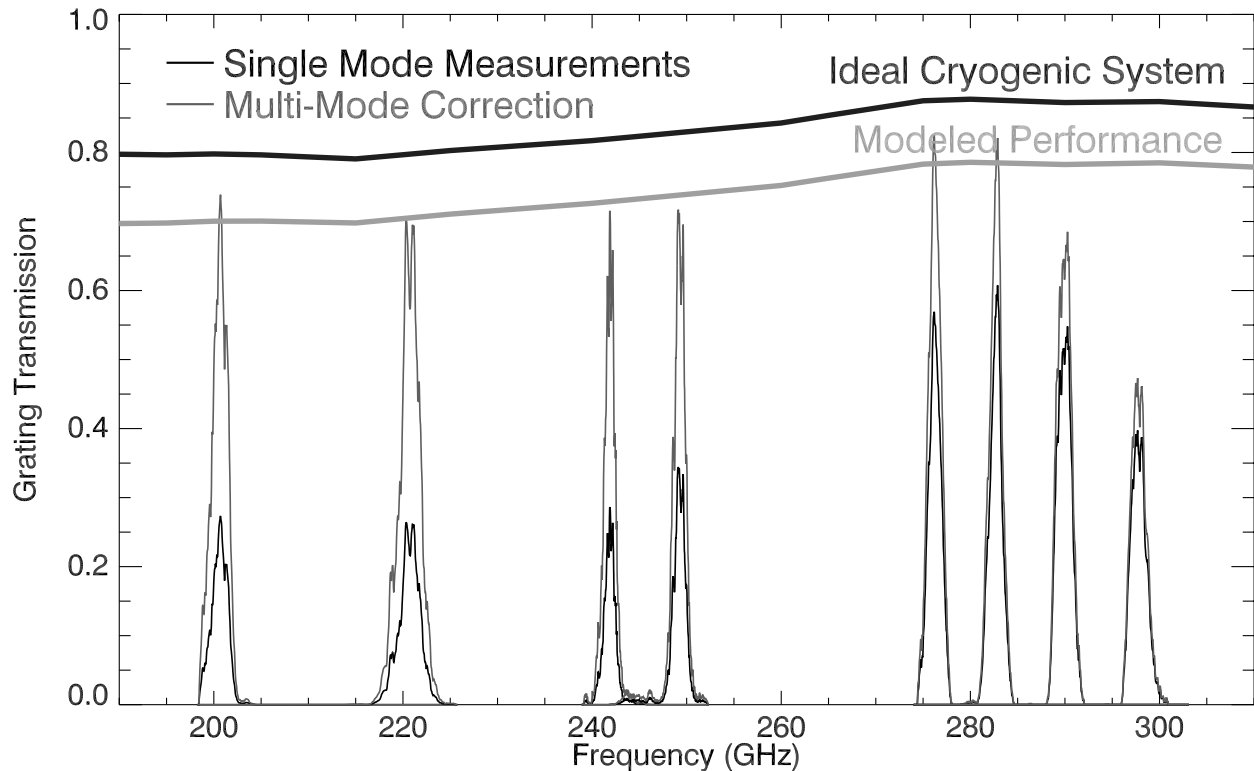


Figure 4: Room temperature measurements of prototype grating performance. See text for a description of the figure.

4. BOLOMETERS AND COUPLING STRUCTURES

Bolometers are thermal detectors limited by fundamental phonon fluctuations, with NEPs of $\sim(4kT^2G)^{1/2}$, where G is the thermal conductivity of the supports and electrical leads⁷. G is tuned for the expected optical loading and bath temperature by adjusting the amount of gold vapor-deposited on one of the Si_3N_4 support legs. The target thermal conductance for the Z-Spec bolometers is 15 pW/K at 100 mK, tailored for the expected millimeter-wave background loading. The designed dark NEPs are $\sim 4 \times 10^{-18} \text{ W Hz}^{-1/2}$ with thermal time constants of 15 ms. Figure 5 shows a bolometer mask designed for Z-Spec.

Z-Spec's 160 detectors are Si_3N_4 micromesh bolometers with neutron-transmutation-doped (NTD) germanium thermistors. The bolometers are etched from silicon wafers 370 microns thick and attached to deep-trenched etched silicon backshorts. Each bolometer/backshort combination is individually mounted on a machined alumina module. The alumina pieces are screwed into the bend blocks which waveguide-couple the outputs of the spectrometer to the bolometers. These blocks have waveguide bends which alternate above or below the plane of the parallel-plate waveguide. This creates maximum space between adjacent bolometers, to make room for readout wires, but eliminates the need for tapering or gaps between the waveguide feeds.

One of the principle challenges of Z-Spec will be realizing high optical efficiency. Therefore, we have carried out detailed numerical simulations of the various interfaces in the Z-Spec grating, including the parallel plate to rectangular waveguide interfaces and the waveguide bends; bolometer absorption simulations are underway. The simulations were done using Ansoft's High Frequency Structure Simulator (HFSS), which simulates the full electromagnetic fields in 3-dimensional structures. This type of simulation has been done for bolometric systems in the past and yielded good agreement with experimental measurements⁸.

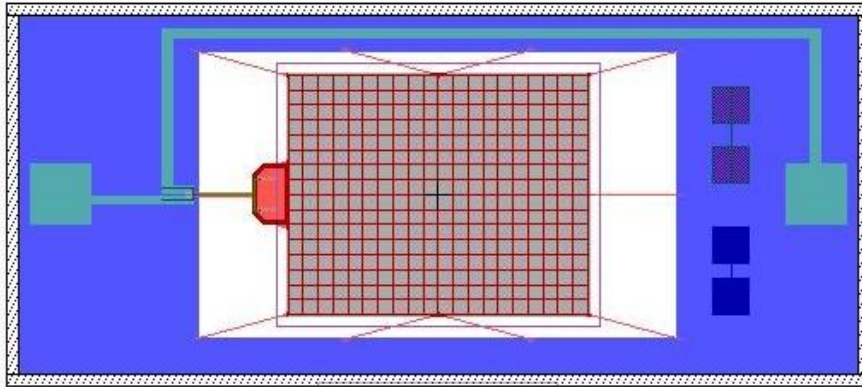


Figure 5: Z-Spec bolometer mask. The Si_3N_4 absorbing mesh is in the center; the filling factor of the grid is a few percent. The square wirebond pads that are vapor deposited on the Si_3N_4 top layer of the wafer can be seen on the left and right.

The rectangular waveguide output feeds in the bend blocks should produce beams in the parallel-plate region that match the incoming radiation patterns from the grating. The focal curve of the grating is a circular arc with its center in the middle of the parallel-plate waveguide. If the feeds were oriented radially along the focal curve, the beams would not couple well to the incoming light from the grating, especially at the low frequencies. Our simulations indicate that the coupling can be optimized by orienting the waveguides at (frequency-dependent) angles ranging from -2° to 28° with respect to the center of the focal arc (see Figure 6a). We confirmed these calculations with warm testing of the prototype spectrometer. While the bolometer feeds are highly overmoded (20-30 possible modes), three modes are sufficient to collect the power from spectral lines landing directly on a single feed or between two adjacent feeds. Figure 6b shows an HFSS simulation of the electric field in a mitre bend. The calculated reflection losses in the bend in the TE_{10} (fundamental mode), $\text{TE}_{11}/\text{TM}_{11}$ (second mode), and $\text{TE}_{12}/\text{TM}_{12}$ modes were 3%, 12%, and 15%, respectively. The bend blocks can be made with either mitred or gently curved waveguide bends. The mitred bends are the more compact, but don't couple as well as the curved bends. We are investigating both options for Z-Spec.

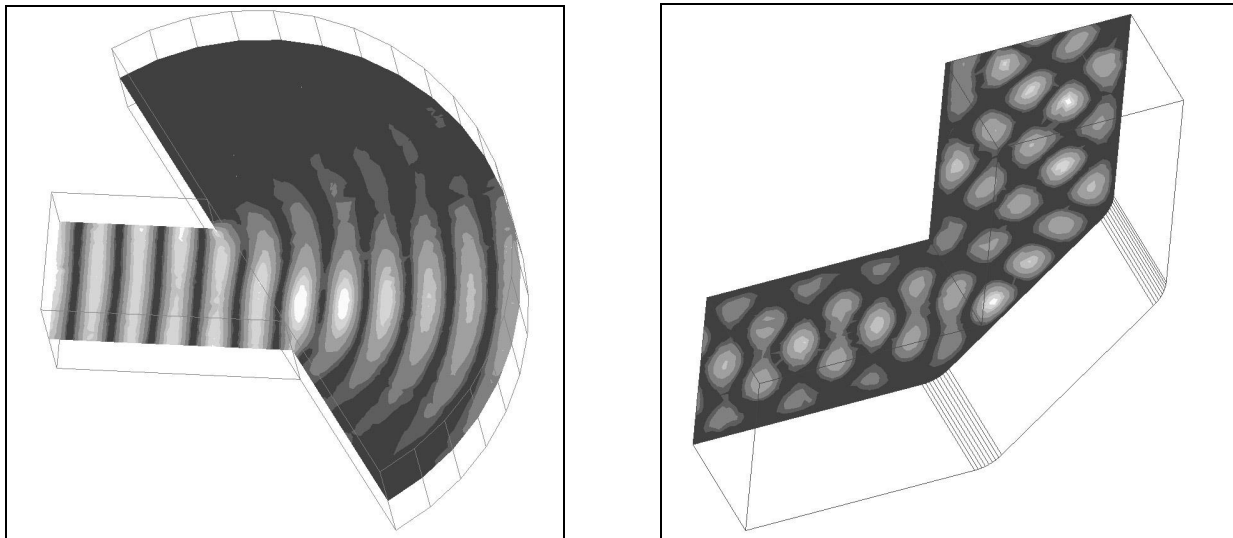


Figure 6: (a – left) HFSS simulation of the beam pattern of a rectangular waveguide feed. The fundamental TE_{10} mode is shown. Light areas correspond to large electric field intensity. The parallel plate region is 2.5 mm tall and the rectangular waveguide feeding into it from the left is 1.8 mm \times 2.5 mm. (b – right) Simulation of the electromagnetic fields in a mitred bend to calculate the reflection loss, the overmoding is apparent. Symmetry was used in this simulation to cut the volume in half; the real dimensions of the waveguide are 3.2 mm \times 2.5 mm. Both simulations were made at 250 GHz.

5. CRYOGENIC DESIGN

Reaching the background limit for a millimeter-wave spectrometer requires detectors cooled to $T \sim 0.1$ K (see Section 4). Furthermore, the optical power incident on a detector from inside the instrument should be small relative to the in-band background power from the sky and telescope. For a detector coupling a fractional bandwidth of $1/300$, the background power at the CSO is $0.2\text{--}0.4$ pW. In comparison, the power coupled by a 2 mm square detector in a 2 K enclosure is 4 pW; hence careful attention must be paid to cryogenics and filtering. In Z-Spec, there are no band-limiting filter elements downstream once the light enters the spectrometer, requiring that the entire spectrometer must be cooled below 1 K.

The cryogenic system for Z-Spec allows for rapid cooling of the massive spectrometer and detectors from room temperature through 2 gas-gap heat switches (Figure 7). Gas-gap switches provide much higher on-stage conduction than mechanical switches; a necessity due to the large 100 mK mass (4 kg of aluminum). We use an adiabatic demagnetization refrigerator (ADR) to achieve the 100 mK base temperature. ADRs have been used to cool detectors in astronomical instruments for several years^{9,10,11}, and offer a somewhat simpler implementation than a dilution refrigerator. Our system uses a ferric ammonium alum (FAA) salt pill for which the entropy is entirely magnetic below about 1.5 K. Upon removing the magnetic field, the entropy available for cooling is approximately $R \ln 6$ per mole of salt, or 7 J / K with our 0.5 mole pill; the entropy of the grating at 1.5 K is only 0.5 J / K. For this reason, we cool the entire spectrometer with the ADR, rather than engineering a thermal break between the spectrometer plates and the detector modules.

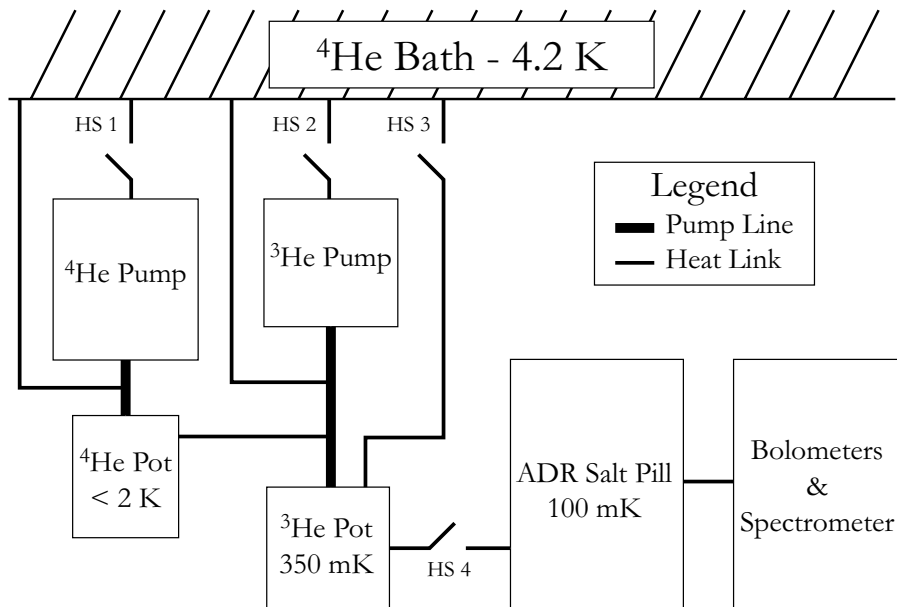


Figure 7: Z-Spec cryogenic design. The spectrometer and bolometers are cooled by an ADR and $^3\text{He} / ^4\text{He}$ sorption refrigerator. The fridge is cycled in stages. First, a magnetic field is applied to the ADR, and HS's 3 & 4 are closed to conduct the heat of magnetization to 4 K. Then ^4He is condensed by opening HS 1 and heating the ^4He pump with a resistive heater. Liquid ^4He condenses in the pump tube at the thermal link and drips into the evaporator. HS 1 is closed to cool the pump, which pumps the liquid ^4He in the ^4He evaporator to < 2 K. The ^3He stage is then cycled by opening HS 3, opening HS 2, and heating the ^3He pump. The ^4He stage condenses liquid ^3He at ~ 2 K, cooling the ADR to 2 K and exhausting the ^4He in the process. The ^3He pump is then cooled by closing HS 2, cooling the ^3He evaporator to 350 mK. During the cooldown to 350 mK, HS 4 is opened and the ADR is demagnetized to 100 mK. The exact timing of the ADR cycle depends on the dissipation of HS 4, the thermal time constant of the ADR and spectrometer, and will be determined empirically.

Once cold, the ADR's entropy overhead would be quickly consumed by the parasitic heat loads from 4 K. A ^3He system is therefore used as a 0.4 K thermal guard, intercepting the heat conducted through the wires, and shielding the large spectrometer surface area from the 4 K radiation. In Z-Spec, the ^3He stage is integrated with a closed cycle ^4He stage, which provides the condensation temperature required for the ^3He , and is used to pre-cool the salt pill and cold stage down to < 2 K before demagnetization. This closed-cycle $^3\text{He} / ^4\text{He}$ combination refrigerator is completely modular, it requires no pumping on the main cryostat bath, and its operation can be fully automated. With the guard in place, the anticipated hold time of the system at 100 mK is around 48 hours and is limited by the ^3He fridge hold time. Images of some components of Z-Spec's cryogenic system are shown in Figure 8. The grating mounting structure has been designed and is shown in Figure 9.

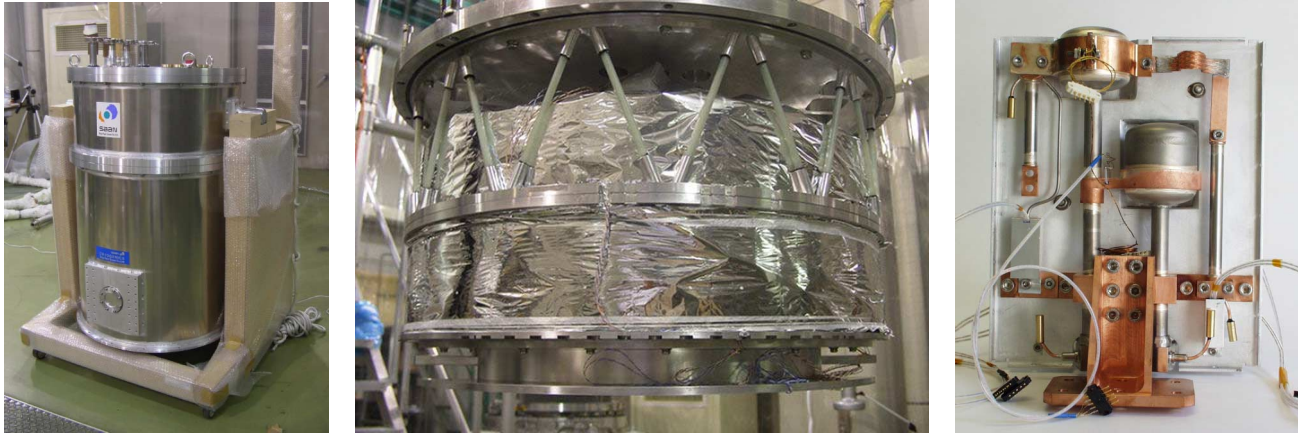


Figure 8: Z-Spec cryogenics. The left photo is an exterior view of the cryostat. The drum head mounting structure of the helium stage is seen in the middle. The closed-cycle $^3\text{He} / ^4\text{He}$ fridge is shown on the right. The pots are shown; the pumps are on the opposite side.

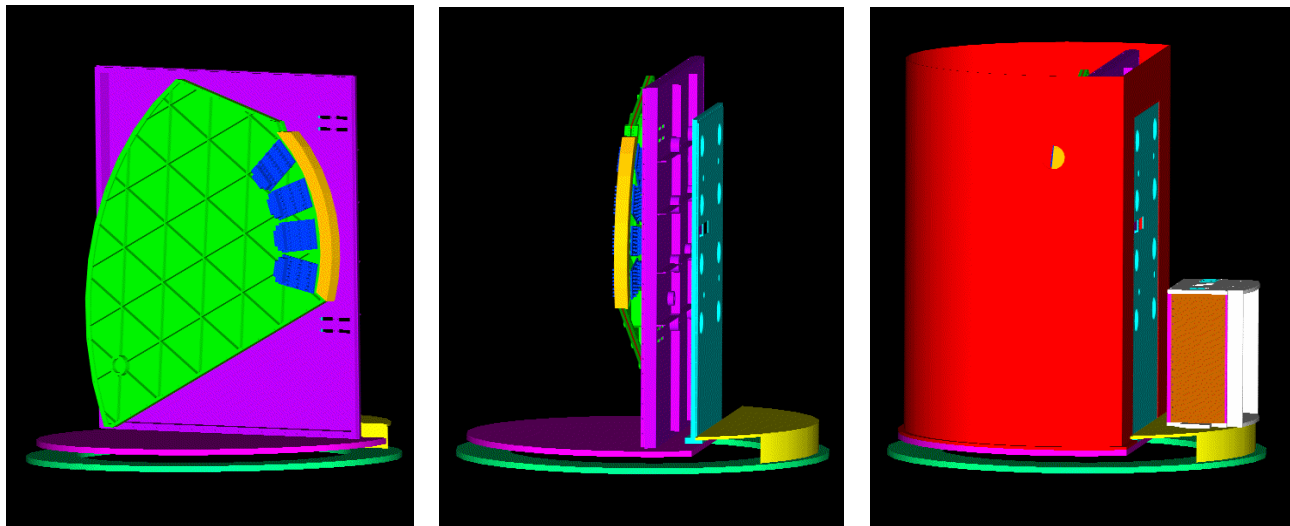


Figure 9: WaFIRS module mounted inside Z-Spec cryostat. The module is isolated from 4 K with a suspension at 400 mK, including a radiation shield completely enclosing the spectrometer (not shown for clarity). At the 400 mK and 100 mK stages, the mechanical support is provided by multiple custom modules in which Kevlar rope is strung between two thermally isolated stages and tensioned with a stack of spring washers. The image on the right shows the 4 K shield enclosing the cold portions, and the J-FET housing mounted on the 77 K cold plate (lower right).

6. GROUND BASED ASTRONOMICAL CAPABILITIES

With sensitive 100 mK bolometers and high throughput, Z-Spec will operate near the fundamental limit set by the fluctuations of the sky and telescope background. Detector sensitivities are expected to be around $4 \times 10^{-18} \text{ W Hz}^{-1/2}$. The noise contribution from the background light in a single diffraction-limited beam can be expressed as

$$NEP_{BG} = h\nu \sqrt{N_{pol} \Delta\nu \bar{n} (\bar{n} + 1)}$$

where \bar{n} refers to the reduced photon occupation number which includes the emissivity of the background radiation ϵ , the coupling through the instrument τ , and the absorption efficiency of the detector η :

$$\bar{n} = \epsilon \tau \eta (1 - \exp(h\nu/kT))^{-1}$$

At the CSO in the 1 mm window, the emissivity of the sky and telescope together can be as low as 15% under very good conditions. We take an instrument transmission and detector efficiency product of 25%, and fold in the bandwidth on a single detector which is

$$\Delta\nu = \frac{\nu}{R} = \frac{\nu^2}{400 \cdot 195 \text{ GHz}} = 1.28 \times 10^4 \nu_{\text{GHz}}^2 \quad [\text{Hz}]$$

The result is an NEP around $1 \times 10^{-17} \text{ W Hz}^{-1/2}$, increasing somewhat with frequency. When combined in quadrature, the detector NEP contributes 15% of the total.

To convert the noise at the detector into an astronomical line flux sensitivity, it is necessary to back out the detector efficiency and instrument transmission, the aperture efficiency of the telescope, its area, and transmission of the sky. Because the instrument band spans a full factor of 1.5 in wavelength, the aperture efficiency can vary substantially over the band, and we include this effect. A factor of 2 is included to account for the detection of only a single polarization, and another factor of 2 accounts for chopping. In addition, we include a factor of sqrt(1.6) since on average, 1.6 detectors will be required to measure a line flux.

At the CSO, an integration time of 6 hours provides a 3σ sensitivity of $4.7 \times 10^{-20} \text{ W/m}^2$, while the much larger IRAM telescope allows integration to 3σ sensitivities of $1.2 \times 10^{-20} \text{ W/m}^2$ in the same time. These sensitivities are sufficient to measure CO lines in the brightest submillimeter galaxies. Figure 10 plots the sensitivity of Z-Spec to a bright submillimeter galaxy as a function of redshift at the CSO. The CO line luminosities are estimated as fractions of the total source based on a model by Maloney et al. (personal communication); the fractions vary from 4×10^{-6} to 5×10^{-5} . The plots show each CO line appearing in the 195-310 GHz band in turn as redshift increases. At least two lines are observable for all redshifts greater than 0.9, which provides an unambiguous redshift measure. For $z < 0.9$, one or two candidate redshifts can be obtained from a single CO line.

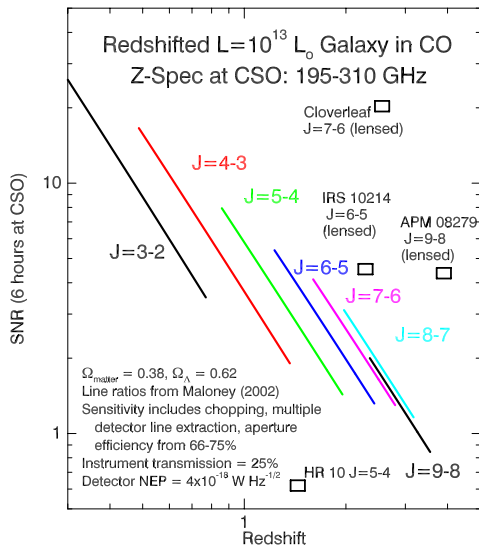


Figure 10: Sensitivity of Z-Spec to a $L = 10^{13} L_{\text{solar}}$ galaxy at the 10.4 m CSO.

7. CONCLUSION

We have described the design of Z-Spec, a direct-detection millimeter-wave spectrometer for use at the CSO. Z-Spec has been designed to provide modest resolving power (250-400) over a broad band in the 1 mm window. With Z-Spec, we will measure the redshifts of bright submillimeter galaxies and probe the millimeter-wave spectra of nearby galaxies, rapidly obtaining a complete census of millimeter-wave coolants. Z-Spec will also demonstrate a spectrometer technology that will enable broadband, background-limited, far-infrared spectroscopy from space.

ACKNOWLEDGEMENTS

We are grateful to Peter Siegel at JPL for his generous help with the prototype spectrometer testing. We would like to acknowledge support from the JPL Directors Research and Development Fund, sponsored by NASA. Jason Glenn also acknowledges NASA (NAGS-11911) and The Research Corporation (RI0928). C. Matt Bradford is supported in part by a Millikan Fellowship at CIT.

REFERENCES

- [1] Puget, J.-L., Abergel, A., Bernard, J.-P., Boulanger, F., Burton, W.B., Desert, F.-X., & Hartmann, D., "Tentative detection of a cosmic far-infrared background with COBE", *A&A*, Vol. 308, L5-L8. 1996
- [2] Hauser, M.G. et al., "The COBE Diffuse Infrared Background Experiment Search for the Cosmic Infrared Background I. Limits and Detections", *ApJ*, Vol. 508, pp. 25-43. 1998
- [3] Fixsen, D.J., Dwek, E., Mather, J.C., Bennett, C.L., & Shafer, R.A., "The Spectrum of the Extragalactic Far-Infrared Background from the COBE FIRAS Observations," *AJ*, Vol. 508, pp. 123-128. 1998
- [4] Blain, A.W., Smail, I., Ivison, R.J., Kneib, J.-P., and Frayer, D.T., "Submillimeter Galaxies", *Physics Reports, in press*. 2002
- [5] Bradford, C.M. et al., "WaFIRS: a waveguide far-IR spectrometer for spaceborne astrophysics", *Proc SPIE*, 4850-162. 2002
- [6] Glenn, J. et al., "Bolocam: a large-format millimeter-wave bolometric camera", *Proc SPIE*, 4855-03, 2002
- [7] Richards, P.L., "Bolometers for infrared and millimeter waves", *J. Appl. Phys.*, Vol. 76, p. 1-24. 1994
- [8] Glenn, J., Chattopadhyay, G., Edgington, S.F., Lange, A.E., Bock, J.J., Mauskopf, P.D., and Lee, A.T., "Numerical Optimization of Integrating Cavities for Diffraction Limited Millimeter-Wave Bolometer Arrays". *Applied Optics*, 41, 136. 2002
- [9] Bradford, C.M. et al., "SPIFI: a direct-detection imaging spectrometer for submillimeter wavelengths", *Applied Optics*, 41 (13): 2561-2574. 2002
- [10] McCammon, D. et al., "A sounding rocket payload for X-ray astronomy employing high-resolution microcalorimeters", *Nuclear Instruments & Methods in Physics Research (A)*, 370 (1), 266-268. 1996
- [11] Ruhl, J., & Dragovan, M., "A Portable 0.050 K Refrigerator for Astrophysical Observations", *Low Temperature Detectors and Dark Matter IV*, eds. N. E. Booth & G. L. Salmon, Editions Frontiers (1991).